

# Phase diagram of imbalanced fermions in optical lattices

Xiaoling Cui and Yupeng Wang

Beijing National Laboratory for Condensed Matter Physics and Institute of Physics,  
Chinese Academy of Sciences, Beijing 100190, China

(Dated: April 16, 2019)

The zero temperature phase diagrams of imbalanced two species fermions in 3D optical lattices are investigated to evaluate the validity of the Fermi-Hubbard model. It is found that depending on the filling factor, s-wave scattering strength and lattice potential, the system may fall into the normal( $N$ ) phase, magnetized superfluid( $SF_M$ ) or phase separation of  $N$  and  $BCS$  state. By tuning these parameters, the superfluidity could be favorable by enhanced effective couplings or suppressed by the increased band gap. The phase profiles for imbalanced fermions in the presence of a harmonic trap are also investigated under LDA, which show some novel structures to those without the optical lattice.

In the past few years, great experimental progresses have been achieved in studying ultracold Fermi gases with polarization<sup>1,2,3,4,5</sup>. With two equal mixtures of cold  ${}^6\text{Li}$  atoms in a harmonic trap<sup>1,2</sup>, a clear evidence of phase separation with an unpolarized superfluid ( $BCS$ ) core and a normal ( $N$ ) shell around that has been observed in experiment. Theoretically<sup>6,7,8,9,10,11,12,13</sup>, many other ground state candidates have been proposed in such systems, including magnetized superfluid ( $SF_M$ ), phase separation ( $PS$ ), and Fulde-Ferrell-Larkin-Ovchinnikov ( $FFLO$ ) state with finite momentum pairing by tuning the interaction parameter  $1/k_F a_s$ , the polarization  $P = \delta n/n$  or zeeman field  $h$ . Since the optical lattice height  $V_0$  is also tunable, it is very interesting to study its effect on the new phase diagram. For equal mixtures, a second-order quantum phase transition between  $SF$  and insulating ( $IN$ ) phase has been addressed both experimentally at a critical lattice height  $V_c$  at resonance<sup>14</sup> and theoretically<sup>15,16</sup> based on the second-order perturbation theory. Besides, there are also works on imbalanced fermions in optical lattices focusing on  $IN$  phase<sup>18</sup> and  $FFLO$  phase<sup>19</sup>, based on an effective Fermi-Hubbard model.

In this work, starting from the exact lattice spectrum, we study the ground state phase diagram of imbalanced two species Fermi gases trapped in 3D optical lattices, in terms of the total filling factor  $n$ , polarization  $P$ , s-wave scattering length  $a_s$  and lattice potential  $V_0$ . Limited by the numerical attainment, the  $FFLO$ -type pairing is not considered. The total pairing reciprocal lattice momentums involved in our simulation are up to the six smallest non-zero ones, which turn out to be more and more important as  $V_0$  increases. Sufficient multiple bands have been taken into account to ensure the accuracy especially in the strong coupling regime. We demonstrate that there are two contradictory effects of  $V_0$  on the superfluid ( $SF$ ) phase, depending on the average filling factor  $n$ . One is the enhanced density of state ( $DOS$ ) inside each band which effectively increases the coupling strength and thus is favorable to  $SF$ ; The other is the broadened band gap or discontinuity of  $DOS$  which is against  $SF$ . One key point is that besides tuning  $a_s$  through the Feshbach

Resonance,  $V_0$  can also be tuned and drive the system from weak to strong coupling regime, provided the filling factor is properly fixed. An obvious evidence is the emergence of  $SF_M$  phase for deep optical lattices at particular filling regimes, even in far  $BCS$  side of Feshbach Resonance. We also propose that the critical polarization versus total filling factor diagram obtained can be used to evaluate the validity of the usual Fermi-Hubbard model. The phase profile in the presence of an external harmonic trap, which is more relevant to the practical experiment will be studied with local density approximation ( $LDA$ ) finally. Some exotic structures appear, reflecting the uniqueness of the optical lattices.

In a recent experiment<sup>14</sup>, two hyperfine states of ultracold  ${}^6\text{Li}$  atoms,  $|F = 1/2, m_F = 1/2\rangle$  ( $|\uparrow\rangle$ ) and  $|F = 1/2, m_F = -1/2\rangle$  ( $|\downarrow\rangle$ ), had been successfully loaded to an optical lattice. The low-energy interactions are characterized by a single s-wave scattering length  $a_s$ , which can be tuned by FR. Such a system can be well described by the one-channel Hamiltonian

$$H = \int d\mathbf{r} \sum_{\sigma=\uparrow,\downarrow} \psi_{\sigma}^{\dagger}(\mathbf{r}) \hat{H}_0(\mathbf{r}) \psi_{\sigma}(\mathbf{r}) + g \int d\mathbf{r} \psi_{\uparrow}^{\dagger}(\mathbf{r}) \psi_{\downarrow}^{\dagger}(\mathbf{r}) \psi_{\downarrow}(\mathbf{r}) \psi_{\uparrow}(\mathbf{r}), \quad (1)$$

where  $\hat{H}_0 = \sum_{i=x,y,z} -\hbar^2 \partial_i^2 / 2M + V_0 \sin^2(\pi x_i / a)$ ;  $a = \lambda/2$  is the period of the lattice generated in each direction by two oppositely propagating lasers with wavelength  $\lambda$ ;  $V_0$  is the lattice height which is usually measured by the recoil energy  $E_R = \hbar^2 \pi^2 / 2M a^2$ ;  $g$  is the renormalized contact interaction constant between the two species by eliminating the unphysical divergence due to the high-momentum contribution for a Fermi gas,  $\frac{1}{g} = \frac{m}{4\pi \hbar^2 a_s} - \frac{1}{V} \sum_q \frac{1}{2\epsilon_q}$ . This approximation approach is reasonable because for rather high-energy with  $\epsilon_{nk} \gg V_0$ , the lattice almost shares the same dispersion relation to that of free Fermi gases.

In the framework of mean-field approach, we expand firstly each field operator in terms of eigen-wavefunctions of  $\hat{H}_0$ ,  $\psi_{\sigma}(\mathbf{r}) = \sum_{\mathbf{nk}} \phi_{\mathbf{nk}}(\mathbf{r}) \psi_{\mathbf{nk}\sigma}$ . The Bloch wavefunc-

tions  $\phi_{\mathbf{n}\mathbf{k}}(\mathbf{r}) = \frac{1}{\sqrt{V}} \sum_{\mathbf{G}} a_{\mathbf{n}\mathbf{k}}(\mathbf{G}) e^{i(\mathbf{k}+\mathbf{G})\cdot\mathbf{r}}$  and energies  $\epsilon_{\mathbf{n}\mathbf{k}}$  are obtained from the Schrödinger equation

$$\sum_{\mathbf{G}'} \left[ \frac{\hbar^2}{2M} (\mathbf{k} + \mathbf{G}')^2 + \frac{3V_0}{2} \delta_{\mathbf{G}\mathbf{G}'} - \frac{V_0}{4} \sum_i \delta_{\mathbf{G}\pm\frac{2\pi}{a}\mathbf{e}_i, \mathbf{G}'} \right] a_{\mathbf{n}\mathbf{k}}(\mathbf{G}') = \epsilon_{\mathbf{n}\mathbf{k}} a_{\mathbf{n}\mathbf{k}}(\mathbf{G}), \quad (2)$$

where  $\mathbf{n} = \{n_x, n_y, n_z\} = s, p, \dots$  indicate the band indices;  $\mathbf{k}$  lie in the first Brillouin Zone (*BZ*) and  $\mathbf{G} = 2\pi/a(l_x, l_y, l_z)$  is the reciprocal lattice vector. The solutions satisfy  $\sum_{\mathbf{G}} a_{\mathbf{n}\mathbf{k}}^*(\mathbf{G}) a_{\mathbf{n}'\mathbf{k}}(\mathbf{G}) = \delta_{\mathbf{n}\mathbf{n}'}$  and  $a_{\mathbf{n}, -\mathbf{k}}(-\mathbf{G}) = a_{\mathbf{n}\mathbf{k}}^*(\mathbf{G})$ . The standard mean-field treatment gives

$$H - \sum_{\sigma} \mu_{\sigma} N_{\sigma} = \sum_{\mathbf{n}\mathbf{k}\sigma} (\epsilon_{\mathbf{n}\mathbf{k}} - \mu_{\sigma}) \psi_{\mathbf{n}\mathbf{k}\sigma}^{\dagger} \psi_{\mathbf{n}\mathbf{k}\sigma} - \sum_{\mathbf{m}, \mathbf{n}} (\Delta_{\mathbf{m}\mathbf{n}\mathbf{k}}^* \psi_{\mathbf{m}-\mathbf{k}\downarrow} \psi_{\mathbf{n}\mathbf{k}\uparrow} + h.c.) - \frac{V}{g} \sum_{\mathbf{Q}} |\Delta_{\mathbf{Q}}|^2, \quad (3)$$

with

$$\Delta_{\mathbf{Q}} = -\frac{g}{V} \sum_{\mathbf{m}\mathbf{n}\mathbf{k}} M_{\mathbf{m}\mathbf{n}\mathbf{k}}^{\mathbf{Q}} \langle \psi_{\mathbf{m}-\mathbf{k}\downarrow} \psi_{\mathbf{n}\mathbf{k}\uparrow} \rangle, \quad (4)$$

$$\Delta_{\mathbf{m}\mathbf{n}\mathbf{k}} = \sum_{\mathbf{Q}} \Delta_{\mathbf{Q}} M_{\mathbf{m}\mathbf{n}\mathbf{k}}^{\mathbf{Q}*},$$

and  $M_{\mathbf{m}\mathbf{n}\mathbf{k}}^{\mathbf{Q}} = \sum_{\mathbf{G}} a_{\mathbf{m}-\mathbf{k}}(-\mathbf{G}) a_{\mathbf{n}\mathbf{k}}(\mathbf{G} + \mathbf{Q})$ . Since  $M_{\mathbf{m}\mathbf{n}\mathbf{k}}^{\mathbf{Q}=0} = \delta_{\mathbf{m}\mathbf{n}}$  and if  $m \neq n$   $M_{\mathbf{m}\mathbf{n}\mathbf{k}}^{\mathbf{Q} \neq 0}$  are quite small, in the following text we only consider pairing within each single band, which means  $\Delta_{\mathbf{m}\mathbf{n}\mathbf{k}} \approx \Delta_{\mathbf{n}\mathbf{k}} \delta_{\mathbf{m}\mathbf{n}}$ . In such a case, the Hamiltonian can be easily diagonalized, and the thermodynamic potential is calculated at  $T = 0$  as

$$\frac{\Omega}{V} = \frac{1}{V} \sum_{\mathbf{n}\mathbf{k}} \{ \Theta(-E_{\mathbf{n}\mathbf{k}\uparrow}) E_{\mathbf{n}\mathbf{k}\uparrow} + \Theta(-E_{\mathbf{n}\mathbf{k}\downarrow}) E_{\mathbf{n}\mathbf{k}\downarrow} + \epsilon_{\mathbf{n}\mathbf{k}} - \mu - \sqrt{(\epsilon_{\mathbf{n}\mathbf{k}} - \mu)^2 + \Delta_{\mathbf{n}\mathbf{k}}^2} \} - \sum_{\mathbf{Q}} \frac{|\Delta_{\mathbf{Q}}|^2}{g}, \quad (5)$$

with  $E_{\mathbf{n}\mathbf{k}\pm} = \sqrt{(\epsilon_{\mathbf{n}\mathbf{k}} - \mu)^2 + \Delta_{\mathbf{n}\mathbf{k}}^2} \mp h$  and  $\mu = (\mu_{\uparrow} + \mu_{\downarrow})/2$ ,  $h = (\mu_{\uparrow} - \mu_{\downarrow})/2$ . From  $\partial\Omega/\partial\Delta_{\mathbf{Q}}^* = 0$  and  $N_{\sigma} = -\partial\Omega/\partial\mu_{\sigma}$ , we get the gap and density equations as

$$-\frac{\Delta_{\mathbf{Q}}}{g} = \frac{1}{V} \sum_{E_{\mathbf{n}\mathbf{k}\pm} > 0} \frac{M_{\mathbf{n}\mathbf{k}}^{\mathbf{Q}} \Delta_{\mathbf{n}\mathbf{k}}}{2\sqrt{(\epsilon_{\mathbf{n}\mathbf{k}} - \mu)^2 + \Delta_{\mathbf{n}\mathbf{k}}^2}}, \quad (6)$$

$$n = \frac{1}{N_L} \left( \sum_{\mathbf{n}\mathbf{k}} 1 - \sum_{E_{\mathbf{n}\mathbf{k}\pm} > 0} \frac{\epsilon_{\mathbf{n}\mathbf{k}} - \mu}{\sqrt{(\epsilon_{\mathbf{n}\mathbf{k}} - \mu)^2 + \Delta_{\mathbf{n}\mathbf{k}}^2}} \right),$$

$$\delta n = \frac{1}{N_L} \left( \sum_{E_{\mathbf{n}\mathbf{k}\uparrow} < 0} 1 - \sum_{E_{\mathbf{n}\mathbf{k}\downarrow} < 0} 1 \right). \quad (7)$$

Here  $N_L$  is the total number of lattice sites,  $n = (N_{\uparrow} + N_{\downarrow})/N_L$  and  $\delta n = (N_{\uparrow} - N_{\downarrow})/N_L$  are the total filling factor and the difference, respectively. Hereafter we scale all the energies in unit of  $E_R$  and the momenta in unit of  $2\pi/a$ .

To make the numerical simulations attainable but still retain the essence of the problem, besides  $\mathbf{Q} = 0$  we consider other six non-zero  $\mathbf{Q}$ :  $(\pm 1, 0, 0), (0, \pm 1, 0), (0, 0, \pm 1)$ . Due to  $M_{\mathbf{n}\mathbf{k}}^{\mathbf{Q}} = M_{\mathbf{n}\pm\mathbf{k}}^{\pm\mathbf{Q}}$  and the isotropy of 3D cubic lattices, all six non-zero  $\mathbf{Q}$  share the same pairing amplitude  $\Delta_1$ . Therefore we get  $\Delta_{\mathbf{n}\mathbf{k}} = \Delta_0 + 2\Delta_1 (M_{\mathbf{n}\mathbf{k}}^{(100)*} + M_{\mathbf{n}\mathbf{k}}^{(010)*} + M_{\mathbf{n}\mathbf{k}}^{(001)*})$ , and two coupled gap equations in terms of  $\Delta_0$  and  $\Delta_1$ . For a realistic numerical simulation, we apply a cutoff momentum  $|q_{\Lambda}| = \frac{3}{2}(1, 1, 1)$  in RG scheme and correspondingly consider the lowest three bands ( $s, p, d$ ) in each direction of lattice spectrum. This truncation allows totally  $n = 54$  atoms per site at most, which is well above the experimental interest as well as ours in this Letter.

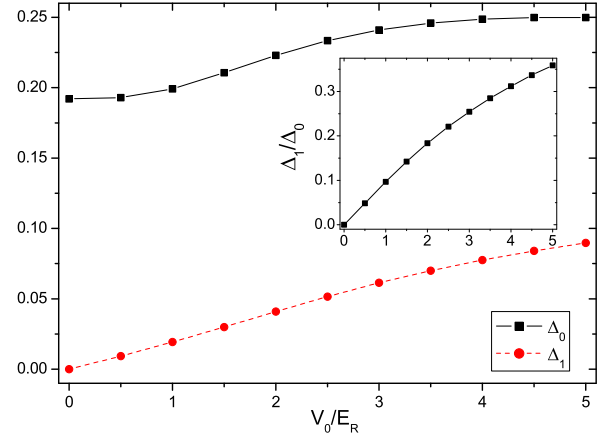


FIG. 1: (color online)  $\Delta_0$ ,  $\Delta_1$  and  $\Delta_1/\Delta_0$  (see inset) vs lattice potentials  $V_0$  for equal mixtures.  $a/a_s = -3$ . The averaged filling is fixed to be  $n = 1$ .

Before turning to the phase diagram of imbalanced system, firstly we analyze the necessity of involving non-zero  $\mathbf{Q}$  in gap equations for equal mixtures. Fig. 1 shows  $\Delta_0, \Delta_1$  and their ratio  $\Delta_1/\Delta_0$  as a function of lattice potential  $V_0$  at half filling  $n = 1$  and  $a/a_s = -3$ . It is shown that the  $\mathbf{Q} \neq 0$  pairing becomes more and more important as  $V_0$  increases. This effect can be understood as follows. Taking a very shallow 1D lattice for example, non-zero  $M_{nk}^{\mathbf{Q}}$  with  $|Q| = 2, 4, 6, \dots$  and  $1, 3, 5, \dots$  only exist around kinetic energy-degenerate points  $k = 0$  and  $k = \pm 1/2$  respectively, which contribute little to gap equations and therefore produce a negligible  $\Delta_1$ . In the limit of  $V_0 = 0$ , these non-zero  $M_{nk}^{\mathbf{Q}}$  exactly cancel with each other in gap equations and finally only  $Q = 0$  pairing survives. However as  $V_0$  increases, the eigen-vector  $a_{nk}(\mathbf{G})$  evolves such that the area of non-zero  $M_{nk}^{\mathbf{Q}}$  expands from three discrete points in first *BZ* to considerable regions around them, leading to an increasing  $\Delta_1$ . The consideration of non-zero  $\mathbf{Q}$ -pairing would produce a much stronger superfluidity especially for deep lattices, which can be seen from the comparison of the previous

two works<sup>17</sup>.

The phase boundaries between  $N$  and  $PS$  (or  $SF_M$ ) at fixed densities can be determined as follows. Firstly solve  $\Delta_{0/1}$  from gap equations for equal mixtures  $\delta n = 0, h = 0$ , and then find the lowest excitation energy  $E_{min} = \text{Min}_{nk}(\sqrt{(\epsilon_{nk} - \mu)^2 + \Delta_{nk}^2})$ , which is also the upper limit of  $h$  ensuring the existence of unpolarized  $BCS$  state. Next  $\Omega_{BCS}(\mu, h = E_{min}, \Delta = \{\Delta_0, \Delta_1\})$  is compared with  $\Omega_N(\mu, h = E_{min}, \Delta = \{0\})$ . If  $\Omega_{BCS} > \Omega_N$  then there must exist a first order phase transition at  $h_c (< E_{min})$  that is determined by

$$\begin{aligned} \Omega_{BCS}(\mu, h_c, \Delta = \{\Delta_0, \Delta_1\}) &= \Omega_N(\mu, h_c, \Delta = \{0\}) \quad (8) \\ n_N(\mu, h_c) &= n. \quad (9) \end{aligned}$$

$P_c = \delta n_N(\mu, h_c)/n$  represents a critical point when  $PS$  is entirely composed by  $N$  phase. In this case, the polarized  $SF$  or Sarma phase<sup>6</sup> is unstable due to the negative superfluid density<sup>11,20</sup>. If  $\Omega_{BCS} < \Omega_N$  then there should be a stable  $SF_M$  interpolating between unpolarized  $BCS$  and polarized  $N$  phase. The upper limit of  $h$  for  $SF_M$ ,  $h_{c2}$ , satisfies the gap equation at  $\Delta_{0/1} = 0$ . Practically,  $\Delta_{0/1}$  can be set to be arbitrarily small in Eq. (7) to obtain  $h_{c2}$ . In free space at the  $SF_M - N$  second-order transition point,  $N$  denotes a fully polarized normal state with  $P_c = 1$ <sup>13</sup>. Correspondingly in optical lattices, we obtain  $P_c = 1$  at  $n \ll 1$  and  $|n - 2|/n$  at  $n \sim 2$ , as shown by red solid circles in Fig. 2.

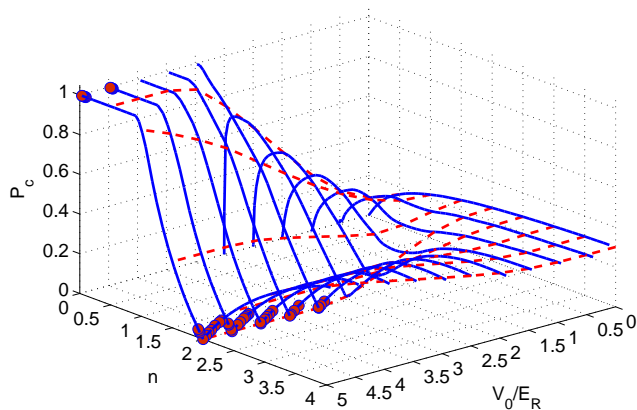


FIG. 2: (color online) Zero temperature phase diagram as a function of polarization  $P_c = \delta n/n$ , total filling factor  $n$  and lattice height  $V_0$ .  $a/a_s = -3$ . The red dashed lines show  $P_c$  evolves with  $V_0$  when the total filling factor is fixed to be  $n = 0.5 \sim 4$ . The blue solid lines show  $P_c$  evolves with  $n$  for optical lattices  $V_0/E_R = 0 \sim 5$ . All the lines above denote the  $PS - N$  boundaries, expect for red solid circles separating  $SF_M$  and  $N$  phase instead.

Fig. 2 shows the ground state phase diagram of imbalanced fermions in cubic optical lattices at  $a/a_s = -3$ , as a function of polarization  $P_c = \delta n/n$ , total filling factor  $n$  and lattice height  $V_0$ .

The  $P_c - V_0$  curves reveal two contradictory effects of increasing  $V_0$  to superfluid phase depending on the filling

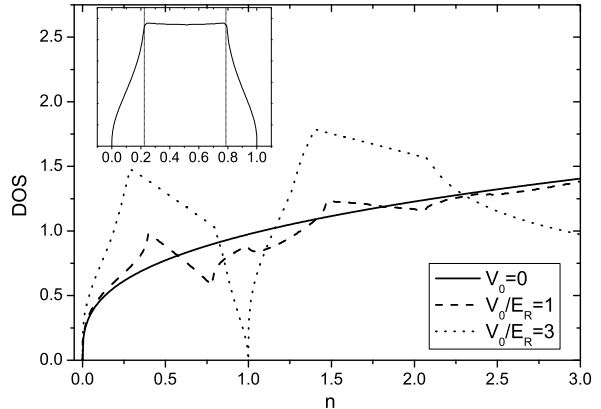


FIG. 3: Density of state( $DOS$ ) at the Fermi surface versus filling factor  $n$  for single-spin atoms in 3D free space and in lattices with  $V_0/E_R = 1$ (no band gap) and  $V_0/E_R = 3$ (with band gap). Inset is  $DOS$  for non-interacting Hubbard model. The dotted lines therein denote two peaks of  $DOS$  at  $(\mu = t, n_p = 0.213)$  and  $(\mu = 3t - \mu, 1 - n_p)$ .

factor  $n$ . As shown in Fig. 3, for  $n \leq 1$  increasing  $V_0$  will make each band flatter and enhance  $DOS$  which is almost inversely proportional to the band width; while at  $n \sim 2$ , increasing  $V_0$  produces an entirely opposite effect due to the enlarged band gap. According to the standard  $BCS$  theory, the  $DOS$  at the Fermi surface dramatically affects the strength of superfluidity. Therefore it is not difficult to understand such contradictory effects. When  $V_0 = 3E_R$ ,  $P_c$  increases to unity at small  $n$  but reduces to zero at  $n = 2$ , denoting the IN phase with  $n_\uparrow = n_\downarrow = 1$ . For  $n \in (1, 2)$ ,  $P_c$  initially drops down and then goes up, indicating the competition between the above two contradictory effects. Here the lattice enhancement of  $P_c$  at  $n \leq 1$  is similar to the enhancement of  $T_c$  for equal mixtures in weak coupling limit<sup>22,23</sup>.

Next we turn to  $P_c - n$  diagram for fixed  $V_0$ . In free space ( $V_0 = 0$ ), as is well known, a first-order phase transition takes place in weak coupling limit at  $h_c = \Delta_0/\sqrt{2}$  and  $P_c = 3h_c/2E_F$ , with the gap amplitude  $\Delta_0 = 8/e^2 E_F \exp(-\pi/2k_F|a_s|)$  and the interaction parameter  $\eta = 1/k_F a_s = \frac{a}{a_s} (3\pi^2 n)^{-1/3}$ . Therefore  $P_c$  increases with  $n$  all along from weak coupling limit ( $\eta \rightarrow -\infty$ ) to the unitary limit ( $\eta \rightarrow 0$ ). Within an optical lattice, however, the  $P_c - n$  curve would be dramatically modified. As explained before, the increasing  $V_0$  will affect the  $DOS$  as well as the effective coupling parameter  $\eta$ . In weak coupling limit with small  $V_0$ , the curve basically follows as that of  $DOS$  in Fig. 3, with a dip at  $n_d \sim 2$  and correspondingly a peak at  $n_p$ . As  $V_0$  increases to drive the system to strong coupling limit, the peak gradually moves to the left and finally vanishes at  $n = 0$ , and finally the stable  $SF_M$  state emerges at  $n \ll 1$  or  $n \sim 2$ . In this limit, two fermions are very likely to form a molecule, and the  $BCS$  equation directly reduces to a Schrodinger equa-

tion for a single bound pair<sup>21,22</sup>. It is expected that as  $V_0$  increases, the  $SF_M$  phase would spread from two small regions ( $n \ll 1$  and  $n \sim 2$ ) to a larger or even the whole region. Actually, the physics at  $n \ll 1$  and  $n \sim 2$  can be related to each other via particle-hole symmetry. The symmetry is essentially obvious within the background of Fermi-Hubbard model,  $\epsilon_{\mathbf{k}} = 0.5t \sum_i (1 - \cos(k_i a))$ . It is easy to check that  $(n, \mu)$  and  $(2 - n, 3t - \mu)$  share the same  $\{\Delta, h, \delta n, \Omega\}$ , and therefore the same critical absolute imbalance  $\delta n_c$ . Based on this fact, the critical polarization  $P_c(n)$  for  $0 < n < 8$  follows

$$P_c = \begin{cases} 1, & n \leq 1 \\ \frac{|n-2|}{n}, & 1 < n \leq 5 \\ \frac{8-n}{n}, & 5 < n \leq 8 \end{cases} \quad (10)$$

We also compute the phase diagram at other s-wave couplings with fixed  $V_0$  as shown in Fig. 4. Compared with Fig. 2, it shows that the increasing  $a/a_s$  always enhance  $SF$  and improve  $P_c$  regardless of the filling factor, which is different from the effect of  $V_0$ . At sufficiently strong coupling close to unitary, it is energetically favorable for particles in s-band to overcome the band-gap and form cooper pairs even at  $n = 2$ . In this case the multi-band effect should be taken into account and the particle-hole symmetry in each band is no longer valid. This is why  $SF_M$  only turns up at  $n \ll 1$  but not at  $n \sim 2$  in unitary limit, shown as the blue circles in Fig. 4.

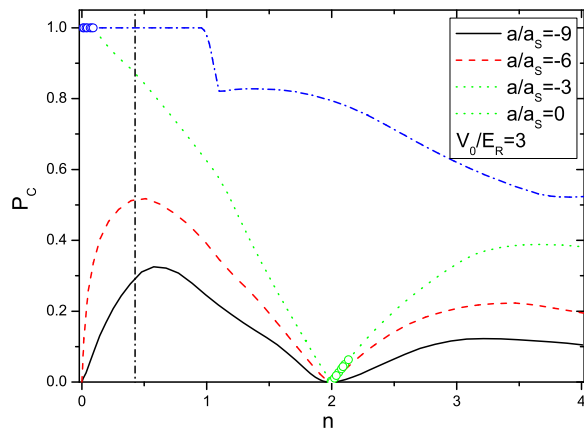


FIG. 4: (color online)  $P_c$  versus  $n$  diagram at different couplings with fixed lattice height  $V_0 = 3E_R$ . Below  $P_c$  it is  $PS$  state, except that the green and blue circles show the  $SF_M-N$  boundaries. The black dashed-dot line marks the upper limit of peak position  $n_p = 0.426$  based on Fermi-Hubbard model.

We emphasize that the  $P_c - n$  diagram in weak coupling limit can be used to evaluate the validity of tight-binding approximation usually applied to the optical lattices. For Hubbard model, the  $DOS$  shows two peaks symmetric around half filling (see inset of Fig. 3), due to the Van Hove singularity at  $(\mu = t, n = 0.213)$  and  $(\mu = 2t, n = 0.787)$ . We also verified numerically that the peak position of  $P_c$  at different couplings is never greater than 0.426 for arbitrary interactions  $|U|/t$ , twice the value as the position of first peak for  $DOS$ . This universal property can be used as a criterion for the validity of tight-binding approximation to realistic lattices. Apparently from Fig. 4 we see that the Fermi-Hubbard model is not applicable to  $V_0 = 3E_R$ , since at really weak coupling ( $a/a_s = -9$ ) the peak position  $n_p \simeq 0.6 > 0.426$ . The disagreement here indicates the deviation of the lattice spectrum from a Hubbard one, and thus the necessity of adopting exact lattice spectrum for not-so-deep lattices.

Finally, it is also useful to consider the  $h - \mu$  phase diagram relevant to realistic experiments with an external harmonic trap. Under  $LDA$ , the system is assumed to be locally homogeneous with an averaged chemical potential  $\mu(\mathbf{r}) = (\mu_{0\uparrow} + \mu_{0\downarrow})/2 - V(\mathbf{r})$  and position-independent difference  $h = (\mu_{0\uparrow} - \mu_{0\downarrow})/2$ , where  $\mu_{0\sigma}$  is the chemical potential for spin- $\sigma$  atoms at trap center. The phase at position  $\mathbf{r}$  is determined by the local  $(\mu(\mathbf{r}), h)$ , which is also self-consistently related to the total particle numbers, s-wave interaction and the lattice potential. Here we give several typical phase profiles with the filling factor in trap center larger than 2. For relatively shallow lattices and very weak s-wave interactions, the most typical phase sequences from the trap center to the edge are:  $BCS-PN-IN-PN-BCS-PN-FN$  ( $PN/FN$ : partially/fully polarized normal phase). Starting from this profile, if  $V_0$  is increased,  $PN$  is very likely to be replaced by  $SF_M$  at positions where  $n(\mathbf{r}) \sim 2$  or  $n(\mathbf{r}) \ll 1$ , while  $IN$  is still expected to exist in a certain region; if s-wave interaction is tuned larger to strong coupling regime,  $IN$  shrinks gradually and two  $BCS$  regimes merge together.  $PN$  gives rise to  $SF_M$ , and eventually there are only three phases left:  $BCS-SF_M-FN$ . In the latter case, much higher bands whose spectrum are nearly continuous would be occupied and very similar to those in free space. The lattice effect is not obvious in this limit.

**Acknowledgments** We thank Fei Zhou and An-Chun Ji for beneficial discussions. X.L. Cui would like to thank the hospitality from UBC during her stay in Canada, where this work is initially started. This work is in part supported by NSFC under grant No. 10574150 and 973-Project(China) under grant No. 2006CB921300.

<sup>1</sup> M. W. Zwierlein, A. Schirotzek, C. H. Schunck, W. Ketterle, *Science* **311**, 492 (2006).

<sup>2</sup> G. B. Partridge, W. Li, R. I. Kamar, Y. Liao, R. G. Hulet,

*Science* **311**, 503 (2006).

<sup>3</sup> M. W. Zwierlein, C. H. Schunck, A. Schirotzek, W. Ketterle, *Nature* **442**, 54 (2006).

- <sup>4</sup> C. H. Schunck, Y. Shin, A. Schirotzek, M. W. Zwierlein, W. Ketterle, *Science* **316**, 867 (2007).
- <sup>5</sup> Y. Shin, C. H. Schunck, A. Schirotzek, W. Ketterle, *cond-mat/07093027*(2007).
- <sup>6</sup> G. Sarma, *J. Phys. Chem. Solids* **24**, 1029 (1963).
- <sup>7</sup> P. Fulde, R. A. Ferrell, *Phys. Rev.* **135**, A550 (1964); A. I. Larkin, Y. N. Ovchinnikov, *Sov. Phys. JETP* **20**, 762 (1965).
- <sup>8</sup> P. F. Bedaque, H. Caldas, G. Rupak, *Phys. Rev. Lett.* **91**, 247002 (2003).
- <sup>9</sup> D. E. Sheehy and L. Radzihovsky, *Phys. Rev. Lett.* **96**, 060401 (2006).
- <sup>10</sup> Z. C. Gu, G. Warner and F. Zhou, *cond-mat/0603091* (2006).
- <sup>11</sup> C. H. Pao, S. T. Wu and S. K. Yip, *Phys. Rev. B.* **73**, 132506 (2006).
- <sup>12</sup> H. Hu and X. J. Liu, *Phys. Rev. A.* **73**, 051603 (2006).
- <sup>13</sup> M. M. Parish, F. M. Marchetti, A. Lamacraft and B. D. Simons, *Nature Physics* **3**, 124 (2007).
- <sup>14</sup> J. K. Chin, D. E. Miller, Y. Liu, C. A. Stan, W. Setiawan, C. Sanner, K. Xu and W. Ketterle, *Nature* **443**, 961 (2006).
- <sup>15</sup> H. Zhai and T. L. Ho, *Phys. Rev. Lett.* **99**, 100402 (2007).
- <sup>16</sup> E. G. Moon, P. Nikolić, and S. Sachdev, *Phys. Rev. Lett.* **99**, 230403 (2007).
- <sup>17</sup> Comparing the previous two works on  $SF - IN$  transition for equal mixtures at resonance, the critical lattice potential  $V_c$  calculated in work<sup>16</sup> is almost one order of magnitude larger than in work<sup>15</sup>, due to the consideration of couplings between different reciprocal lattice vectors.
- <sup>18</sup> M. Iskin and C.A.R. Sá de Melo, *Phys. Rev. Lett.* **99**, 080403 (2007).
- <sup>19</sup> T.K. Koponen, T. Paananen, J.-P. Martikainen, P. Torma, *Phys. Rev. Lett.* **99**, 120403 (2007); T.K. Koponen, T. Paananen, J.-P. Martikainen, M.R. Bakhtiari, P. Torma, *New Journal of Physics* **10**, 045104 (2008).
- <sup>20</sup> S. T. Wu and S. Yip, *Phys. Rev. A.* **67**, 053603 (2003).
- <sup>21</sup> P. Nozières and S. Schmitt-Rink, *Journal of Low Temperature Physics*, **59**, 195 (1985).
- <sup>22</sup> R. Micnas, J. Ranninger, S. Robaszkiewicz, *Rev. Mod. Phys.* **62**, 113 (1990).
- <sup>23</sup> W. Hofstetter, J. I. Cirac, P. Zoller, E. Demler and M. D. Lukin, *cond-mat/0204237*(2002).